Original Article

Mol Imaging Radionucl Ther **DOI:***10.4274/mirt.galenos.2026.23334*

[Epub Ahead of Print]

Evaluation of Cavitary Lung Lesions with ^{18}F-FDG PET/CT: Differentiating Benign from Malignant Lesions

^{18}F-FDG PET/BT ile Kaviter Akciğer Lezyonlarının Değerlendirilmesi: Benign ve Malign Lezyonların Ayırt Edilmesi

Nur Aydınbelge Dizdar[1], Ebru Tatcı[1], Ülkü Nur Derya[2], Özlem Özmen[1]

[1]*University of Health Sciences Türkiye, Ankara Etlik City Hospital, Clinic of Nuclear Medicine, Ankara, Türkiye*
[2]*University of Health Sciences Türkiye, Ankara Atatürk Sanatorium Training and Research Hospital, Clinic of Nuclear Medicine, Ankara, Türkiye*

Abstract

Objectives: This study aimed to analyze ^{18}F-fluorodeoxyglucose positron emission tomography/computed tomography (^{18}F-FDG PET/CT) features to differentiate benign from malignant pulmonary cavitary lesions.

Methods: A total of 76 patients with cavitary lung lesions who underwent ^{18}F-FDG PET/CT imaging were retrospectively analyzed. Patient demographics, histopathological findings, cavitary lesion morphology, CT characteristics, and maximum standard uptake value (SUV_{max}) of lesions were recorded. Cavitary lesions were classified as benign or malignant and further subdivided by maximum wall thickness into two groups: ≤15 mm and >15 mm. Histopathological results, clinical follow-up, or both were used as the reference standard for lesion classification.

Results: Among 76 patients (mean age, 63.4 years), 31 (40.8%) had benign disease and 45 (59.2%) had malignant disease. Malignant lesions were observed at older ages and exhibited significantly greater lesion size, wall thickness, and SUV_{max} than those in benign lesions ($p<0.05$ for all). There were no significant differences between the malignant and benign groups regarding sex, lesion localization, air-fluid levels, or pleural effusion ($p>0.05$ for all). Peripheral consolidation, multiple cavitary lesions, and tree-in-bud pattern were significantly more prevalent in benign lesions than in malignant lesions ($p<0.05$ for all). In lesions with a maximum wall thickness ≤15 mm, SUV_{max} was significantly higher in malignant lesions than in benign lesions (mean values, 9.81 vs. 5.28; $p<0.05$). Malignant lesions with a maximum wall thickness >15 mm demonstrated higher SUV_{max} values (mean 18.37 vs. 10.45; $p<0.05$). SUV_{max} was independently associated with malignancy (odds ratio: 1.237, $p=0.017$) and showed the best diagnostic performance (area under the curve=0.866; cut-off 8.58, sensitivity 80%, specificity 77%).

Conclusion: The morphological characteristics of pulmonary cavitary lesions, associated parenchymal findings, and ^{18}F-FDG uptake patterns on PET/CT provide valuable information for distinguishing between benign and malignant lesions. In this study, SUV_{max} demonstrated the highest diagnostic performance. The combined evaluation of metabolic and morphological parameters can enhance diagnostic accuracy and support the clinical decision-making process, thereby contributing to the optimal management of patients.

Keywords: ^{18}F-FDG PET/CT, cavitary lung lesions, wall thickness, lung cancer, differential diagnosis, SUV_{max}

Address for Correspondence: Nur Aydınbelge Dizdar, University of Health Sciences Türkiye, Ankara Etlik City Hospital, Clinic of Nuclear Medicine, Ankara, Türkiye
E-mail: fnuraydinbelge@gmail.com **ORCID ID:** orcid.org/0000-0002-9657-6906
Received: 23.12.2025 **Accepted:** 29.05.2026 **Epub:** 13.07.2026

Cite this article as: Aydınbelge Dizdar N, Tatcı E, Derya ÜN, Özmen Ö. Evaluation of cavitary lung lesions with ^{18}F-FDG PET/CT: differentiating benign from malignant lesions. [Epub Ahead of Print]

Öz

Amaç: Bu çalışma, benign ve malign pulmoner kaviter akciğer lezyonlarını ayırt etmede ^{18}F-florodeoksiglukoz pozitron emisyon tomografisi/bilgisayarlı tomografi (^{18}F-FDG PET/BT) özelliklerini analiz etmeyi amaçladı.

Yöntem: ^{18}F-FDG PET/BT görüntüleme yapılan toplam 76 kaviter akciğer lezyonu olan hasta retrospektif olarak analiz edildi. Hastaların demografik özellikleri, histopatolojik bulguları, kaviter lezyon morfolojisi, BT özellikleri ve lezyonların maksimum standart tutulum değeri (SUV_{max})'ı kaydedildi. Kaviter lezyonlar benign veya malign olarak sınıflandırıldı ve maksimum duvar kalınlığına göre ≤15 mm ve >15 mm olmak üzere iki gruba ayrıldı. Histopatolojik sonuçlar ve/veya klinik takip, lezyon sınıflandırması için referans standardı olarak kullanıldı.

Bulgular: Toplam 76 hastanın (ortalama yaş: 63,4), 31'i (%40,8) benign hastalık, 45'i (%59,2) malign hastalık tanısı aldı. Malign lezyonlar daha ileri yaşlarda gözlendi ve benign lezyonlara göre anlamlı olarak daha büyük lezyon boyutu, duvar kalınlığı ve SUV_{max} değerleri bulundu (tümü için p<0,05). Cinsiyet, lezyon lokalizasyonu, hava-sıvı seviyelerinin varlığı veya plevral efüzyon açısından gruplar arasında anlamlı bir fark bulunmadı (tümü için p>0,05). Periferik konsolidasyon, çoklu kaviter lezyonlar ve tomurcuklanmış ağaç paterni benign lezyonlarda anlamlı olarak daha sık gözlendi (tümü için p<0,05). Maksimum duvar kalınlığı ≤15 mm olan lezyonlarda, SUV_{max} malign lezyonlarda benign lezyonlara göre anlamlı olarak daha yüksekti (ortalama değerler, 9,81'e karşı 5,28; p<0,05). Maksimum duvar kalınlığı >15 mm olan lezyonlarda, malign lezyonlar benign lezyonlara kıyasla daha yüksek SUV_{max}'a sahipti (ortalama değerler, 18,37'ye karşı 10,45; p<0,05). SUV_{max}, malignite ile bağımsız olarak ilişkili bulundu (olasılık oranı: 1,237, p=0,017) ve en iyi tanısal performansı gösterdi (eğri altında kalan alan=0.866; kesim değeri 8,58, duyarlılık %80, özgüllük %77).

Sonuç: Kaviter akciğer lezyonlarının morfolojik özellikleri, eşlik eden parankimal bulgular ve PET/BT'deki ^{18}F-FDG tutulum paternleri benign ve malign lezyonların ayırt edilmesinde önemli bilgiler sağlamaktadır. Bu çalışmada SUV_{max} en yüksek tanısal performansı göstermiştir. Metabolik ve morfolojik parametrelerin birlikte değerlendirilmesi tanısal doğruluğu artırarak klinik karar verme sürecine ve hasta yönetiminin optimize edilmesine katkı sağlayabilir.

Anahtar Kelimeler: ^{18}F-FDG PET/BT, kaviter akciğer lezyonları, duvar kalınlığı, akciğer kanseri, ayırıcı tanı, SUV_{max}

Introduction

A cavitary lung lesion is a gas-filled space within a pulmonary consolidation, mass, or nodule. The evacuation of necrotic tissue through the bronchial tree leads to the development of cavitation (1). Cavities can develop from a variety of causes, including malignancies (such as squamous cell carcinoma, adenocarcinoma, and small cell lung cancer), infections (such as Streptococcus pneumoniae, Streptococcus aureus, typical and atypical mycobacteria, fungal infections, and parasites), autoimmune diseases (including rheumatoid arthritis or granulomatosis with polyangiitis), sarcoidosis, pulmonary embolism, and congenital abnormalities (such as bronchogenic cyst, pulmonary sequestration, congenital pulmonary airway malformation) (2).

Radiographic differentiation between malignant and benign cavitary lesions is crucial in clinical practice, as it guides management and treatment decisions. Computed tomography (CT) plays significant role in the detection and differential diagnosis of cavitary lesions. The size, shape, location, and wall characteristics of cavitary lesions can provide important clues to their underlying etiology. The thickness of the cavity wall is the most important criterion for assessing these lesions, as it often helps distinguish malignant from benign etiologies. Several studies indicate that malignant cavitary lesions have thicker walls, whereas thin-walled cavitary lesions are usually benign (3,4,5). However, there is no consensus on the CT threshold for wall thickness. Additionally, there may be considerable overlaps in wall thickness between malignant and benign lesions. ^{18}F-fluorodeoxyglucose positron emission tomography with CT (^{18}F-FDG PET/CT) is an important imaging technique for differentiating benign from malignant lung lesions. Moreover, ^{18}F-FDG PET/CT can be useful in evaluating disease severity, identifying optimal biopsy sites, and monitoring treatment response in benign lung diseases such as tuberculosis and sarcoidosis (6). Malignant lesions typically exhibit high ^{18}F-FDG uptake due to increased glycolytic activity. However, ^{18}F-FDG uptake can also be observed in a variety of inflammatory and infectious disorders, including tuberculosis, pneumonia, abscesses, sarcoidosis, and autoimmune diseases, due to increased metabolic activity. Accordingly, this study evaluated ^{18}F-FDG PET/CT imaging features to differentiate benign from malignant cavitary lung lesions based on metabolic and morphological characteristics.

Materials and Methods

Clinicopathological Characteristics of the Patients

In this study, patients who had cavitary lung lesions on radiological exams and underwent ^{18}F-FDG PET/CT for differential diagnosis between 2020 and 2021 at our department were involved. Exclusion criteria included patients with cavitary lesions who had received antibiotic, antiviral, or antifungal therapy prior to ^{18}F-FDG PET/CT, as well as those with incomplete clinical records or suboptimal PET/CT images. Patients with a primary malignancy or a history of granulomatous, rheumatological, or congenital diseases were excluded from the study.

Cavitary lesions were classified primarily into two groups:benign and malignant.The definitive diagnosis was confirmed by sputum and blood culture results, response to treatment, and histopathological findings. Ethical approval for this retrospective study was obtained from the Local Ethics Committee of the University of Health Sciences Türkiye, Ankara Atatürk Sanatorium Training and Research Hospital, (approval no: 661, date: 06.02.2020).

^{18}F-FDG PET/CT Imaging

Prior to the imaging procedure, all patients fasted for 4-6 hours. After confirming that their blood glucose levels were under 190 mg/dL, an average ^{18}F-FDG dose of 390.8±54.2 MBq (ranging from 310 to 565 MBq) was administered intravenously. Sixty minutes after ^{18}F-FDG administration, whole-body PET/CT imaging from the vertex to the proximal femur was performed for each patient using a Siemens Biograph 6 HI-REZ integrated PET/CT scanner (Siemens Medical Solutions, Knoxville, TN, USA). CT scans were first obtained at 130 kV with automatic real-time amperage modulation, a slice thickness of 0.5 cm, a rotation time of 0.6 seconds, a table speed of 1.5 cm per rotation, and a pitch of 1.5. Following CT acquisition, PET images were acquired for 3 minutes per bed position. PET images were attenuation-corrected using the CT data and reconstructed with the ordered-subsets expectation maximization algorithm, employing 4 iterations and 8 subsets. A gaussian post-filter was applied, resulting in a transaxial spatial resolution of 5 mm at full width at half maximum. Reconstructed transaxial, coronal, and sagittal PET, CT and fused PET/CT images, as well as maximum-intensity projection images, were reviewed on a dedicated workstation for visual and semi-quantitative analysis.

Visual assessment was performed to evaluate ^{18}F-FDG uptake relative to background lung activity. Semi-quantitative analysis was performed by placing a region of interest (ROI) over each cavitary lesion to measure the maximum standard uptake value (SUV_{max}). The ROI was carefully drawn to include only the cavitary lesion, excluding any adjacent parenchymal abnormalities, such as consolidation or tree-in-bud patterns. CT morphological features, including cavity wall thickness, the longest axial diameter, and adjacent parenchymal findings, were also recorded. Based on CT findings, the patients were retrospectively classified into probable benign and probable malignant groups. The presence of a tree-in-bud pattern or multiple cavitary lesions on CT imaging was accepted as a criterion for benignity. Additionally, cavitary lesions were subdivided into two groups based on maximum wall thickness: ≤15 mm and >15 mm. The images were evaluated by two nuclear medicine specialists with over 10 years of experience (OO and ET). Any discrepancies between reviewers were resolved by consensus.

Statistical Analysis

Statistical analyses were conducted with SPSS version 27.0 (IBM Corp., Armonk, NY, USA). The relationships between categorical variables were analyzed using the chi-square test, and correlations were evaluated using appropriate correlation methods. The Mann-Whitney U test was used for pairwise comparisons between groups. Spearman correlation analysis was used to assess the associations among SUV_{max}, lesion diameter, and maximum wall thickness. ROC analysis was performed to evaluate the diagnostic performance of SUV_{max}, maximum wall thickness, and lesion diameter, and to determine their optimal cut-off values for differentiating malignant from benign lesions. Logistic regression analysis was used to determine factors associated with malignancy risk. A p-value less than 0.05 was considered statistically significant throughout the analysis.

Results

Clinicopathological Characteristics of the Patients

A total of 76 patients who underwent ^{18}F-FDG PET/CT scan for the assessment of cavitary lesions were enrolled in the study, comprising 10 females (13.1%) and 66 males (86.8%), with a mean age of 63.4±12.7 years. The clinicopathological characteristics of the patients were presented in Table 1. Of the 76 patients, 31 (40.8%) had benign lesions and 45 (59.2%) had malignant lesions. Sex distribution did not differ significantly between the benign and malignant groups (p=0.081). The mean age was significantly lower in the benign group compared with the malignant group (31±12.2 vs. 45±11.8 years, p<0.001). Furthermore, the final diagnoses of benign and malignant cavitary lesions were summarized in Table 2.

^{18}F-FDG PET/CT Findings

No significant differences were detected between benign and malignant cavitary lesions with respect to lung side, presence of air-fluid levels, pleural effusion, and perilesional infiltration (p=0.91, p=0.58, p = 0.66, p=0.13, respectively; Table 3). Malignant cavitary lesions had significantly greater diameters than benign cavitary lesions (p=0.003). Consolidation associated with the primary lesion was more common in benign lesions (p=0.025). The perilesional tree-in-bud pattern was observed in only 8 (25.8%) of the 31 benign lesions. The tree-in-bud appearance was not associated with malignant cavitary lesions. Additional cavitary lesions in the same or the contralateral lung were observed in 8 (25.8%) of 31 benign lesions (Figure 1),

Table 1. Demographic characteristics and the final clinical classification of patients with benign and malignant cavitary lung lesions			
Definitive diagnosis	**Benign (n=31, 40.8 %)**	**Malignant (n=45, 59.2%)**	**p**
Demographic data			
Gender (male/female)	24/7	42/3	0.081
Age (years), mean ± SD (range)	31±12.2 (31-91)	45±11.8 (33-95)	<0.001
Chi-square test for categoric variables, p<0.05 level is significant, Mann-Whitney U test for continuous variable, mean ± SD, p<0.05 level is significant, SD: Standard deviation			

Table 2. Diagnosis of cavitary lung lesions		
Definitive diagnosis	**n**	**%**
Benign	31	
Bacterial abscesses	17	54.8
Tuberculosis	12	38.7
Bronchogenic cyst	1	3.2
Aspergillus infection	1	3.2
Malign	45	
Lymphomatoid granulomatosis	2	4.4
Squamous cell carcinoma	35	78
Carcinoid tumor	1	2.2
Adenocarcinoma	3	6.6
Adenosquamous carcinoma	3	6.6
Small cell lung cancer	1	2.2
Total	76	

whereas no additional cavitary lesions were identified in malignant cavities.

When the presence of multiple cavitary lesions or a tree-in-bud pattern on CT scans was considered a benign imaging feature and was interpreted in conjunction with clinical findings, the preliminary clinical assessment classified 16 of the 76 patients as possibly benign and 60 as possibly malignant (Table 3). All patients (n=16) in the possibly benign group were eventually diagnosed with benign disease. In the group classified as possibly malignant, malignant disease was confirmed in 45 patients (75%), whereas benign lesions were identified in 15 patients (25%).

The mean maximum wall thickness in the malignant cavitary lesions (21.2±9.2 mm, range 6-50 mm) was significantly greater than that of the benign cavitary lesions (12.6±6.2, range 3-27 mm),(p<0.001; Table 3). Only one cavitary lesion had a maximum wall thickness of less than 4 mm, and it was an infectious cavity. The maximum wall thickness was at least 4 mm in all 45 malignant lesions. Of the 76 patients, 36 (47.4%) had a maximum wall thickness ≤15 mm, while 40 (52.6%) had a wall thickness >15 mm (Table 3). Of the 36 cavitary lesions with a maximum wall thickness ≤15 mm, 23 (63.88%) were benign (Figure 2). The remaining 13 lesions (36.12%) were malignant (Figure 3). Of the 40 cavitary lesions with a maximum wall thickness over 15 mm, 8 (20%) were classified as benign and 32 (80%) were classified as malignant (Figure 4). The proportion of malignant lesions was significantly higher in cavitary lesions with a maximum wall thickness >15 mm compared with those ≤15 mm (p<0.001; Table 4). Of the 76 patients, 35 (46.1%) had cavitary lesions with a maximum wall thickness of 5-15 mm. Among the 35 cavitary lesions with a maximum wall thickness of 5-15 mm, 22 (62.9%) were benign and 13 (37.1%) were malignant.

Relationship Between SUV_{max}, Maximum Wall Thickness and Lesion Size

Table 4 shows SUV_{max} by maximum wall thickness and lesion status (benign or malignant) based on the final diagnosis. The SUV_{max} of benign lesions was significantly lower than that of malignant lesions, with mean values of 6.62±4.2 (range: 1.7-21.4) and 15.9±7.6 (range: 4.3-30.3), respectively (p<0.001). According to maximum wall thickness, the overall mean ± standard deviation (SD) of SUV_{max} was 6.92±5.15 in lesions with a wall thickness ≤15 mm and 16.78±6.95 in those with a wall thickness >15 mm. A moderate positive correlation was found between SUV_{max} and the longest axial diameter of the cavitary lesions (r=0.519, p=0.0001; Figure 5). A positive correlation between the maximum wall thickness and SUV_{max} was also observed (r=0.602, p=0.0001).

Univariate and Multivariate Logistic Regression Analyses in Predicting Malign Cavitary Lesion

In univariate logistic regression analysis, increasing age [odds ratio (OR): 1.067, 95% confidence interval (CI): 1.021-1.116, p=0.004], larger lesion diameter (OR: 1.029, 95% CI: 1.007-1.051, p=0.01), greater maximum wall thickness (OR: 1.15, 95% CI: 1.066-1.246, p<0.001), and higher SUV_{max} (OR: 1.316, 95% CI: 1.153-1.502, p<0.001; Table 5) were significantly associated with increased odds of malignancy. In contrast, perilesional consolidation was inversely associated with malignancy

Table 3. The CT findings between benign and malignant cavitary lung lesions based on the final diagnosis			
CT findings	**Benign (n=31, 40.8 %)**	**Malignant (n=45, 59.2%)**	**p**
Localization (left/right lung)	12/19	18/27	0.911
Lesion diameter (mm), mean ± SD (range)	48.5±26 (13-120)	64.6±23.5 (20-120)	**0.003**
Maximum wall thickness (mm), mean ± SD (range)	12.6±6.2 (3-27)	21.2±9.7 (6-50)	**<0.001**
Maximum wall thickness <4 mm, n (%)	1 (1.3%)	0	
Maximum wall thickness 5-15 mm, n (%)	22 (28.9%)	13 (17.1%)	
Maximum wall thickness >15 mm, n (%)	8 (10.5%)	32 (42.1%)	
Presence of air-fluid level, n (%)	9 (11.8%)	17 (22.4%)	0.587
Presence of multiple cavitary lesions, n (%)	8 (10.5%)	0	**<0.001**
Presence of pleural effusion, n (%)	12 (15.8%)	14 (18.4%)	0.661
Presence of perilesional consolidation, n (%)	22 (28.9%)	19 (25%)	**0.025**
Presence of perilesional infiltration, n (%)	16 (21.1%)	32 (42.1%)	0.136
Presence of tree-in-bud pattern, n (%)	8 (10.5%)	0	**<0.001**
Preliminary diagnosis based on CT findings Possibly benign Possibly malign	 16 (21.1%) 15 (19.7%)	 0 45 (59.2%)	**<0.001**

Chi-square test for categoric variables, p<0.05 level is significant, Mann-Whitney U test for continuous variables, mean ± SD, p<0.05 level is significant, SD: Standard deviation, CT: Computed tomography

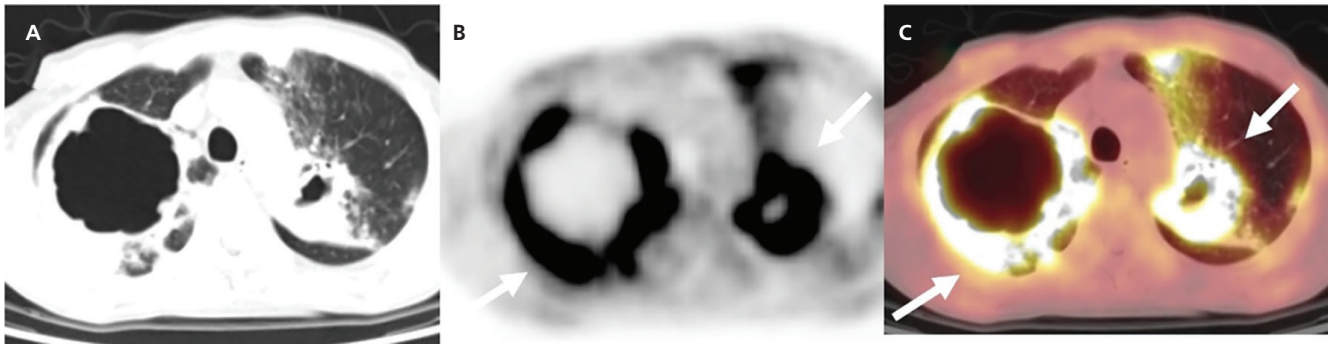

Figure 1. Tuberculosis. Axial CT (A), ^{18}F-FDG PET (B), and fusion PET/CT (C) images show irregular, thick-walled cavitary lesions surrounded by infiltrated pulmonary parenchyma in both lungs, with the largest lesion located in the right apical region measuring approximately 85 mm (arrows). Increased metabolic activity is observed along the cavity walls (SUV_{max}: 14.34)
^{18}F-FDG PET/CT: ^{18}F-fluorodeoxyglucose positron emission tomography/computed tomography, SUV_{max}: Maximum standard uptake value

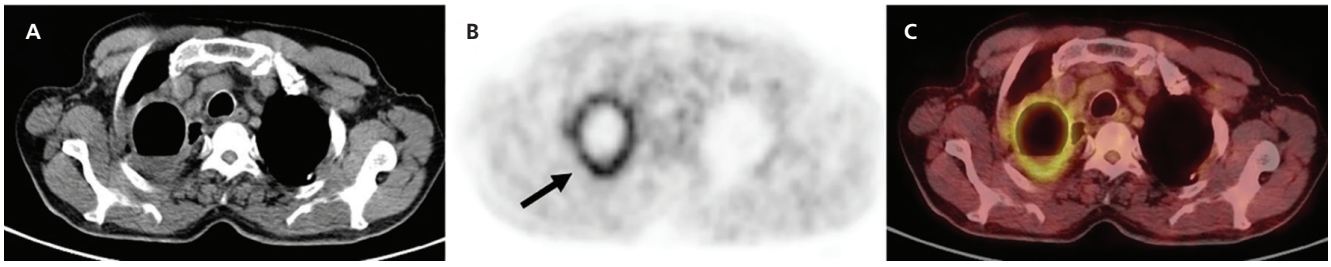

Figure 2. Tuberculosis. Axial CT (A), ^{18}F-FDG PET (B), and fused PET/CT images demonstrate increased ^{18}F-FDG uptake in a cavitary mass lesion containing fluid, measuring approximately 63 mm in diameter, with a maximum wall thickness of 15 mm and SUV_{max} of 8.52 (arrows)
^{18}F-FDG PET/CT: ^{18}F-fluorodeoxyglucose positron emission tomography/computed tomography, SUV_{max}: Maximum standard uptake value

(OR: 0.299, 95% CI: 0.113-0.793, p=0.015), indicating lower odds of malignancy. The presence of air-fluid level, pleural effusion, and perilesional infiltration was not associated with malignancy.

In multivariate analysis, increasing age (OR: 1.071, 95% CI: 1.008-1.137, p=0.025) and higher SUV_{max} (OR: 1.237, 95% CI: 1.039-1.473, p=0.017) remained independently associated with increased odds of malignancy. Conversely, the presence of perilesional consolidation remained independently associated with lower odds of malignancy (OR: 0.142, 95% CI: 0.018-0.649, p=0.029). Other parameters were not associated with malignancy in the multivariate model.

ROC Analysis for Diagnostic Performance

ROC analysis showed that SUV_{max} had the highest diagnostic performance [area under the curve (AUC)=0.866, 95% CI: 0.786-0.947, p<0.001], followed by maximum wall thickness (AUC=0.780, 95% CI: 0.676-0.884, p<0.001) and lesion diameter (AUC=0.701, 95% CI: 0.574-0.828, p=0.003; Figure 6). The optimal cut-off values to differentiate malignant from benign lesions were 53.5 mm for lesion size (66% sensitivity, 64.5% specificity), 15.5 mm for maximum wall thickness (71.1% sensitivity, 74.2% specificity), and an SUV_{max} of 8.58 (80% sensitivity, 77% specificity).

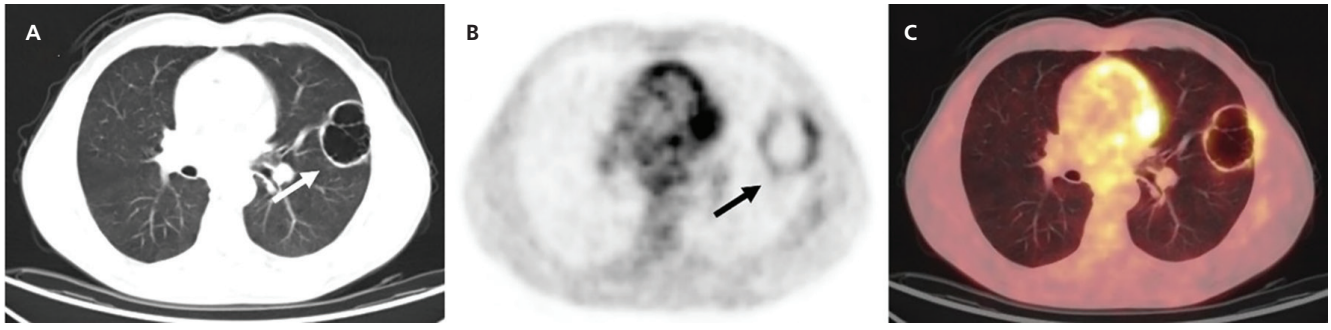

Figure 3. Squamous cell carcinoma. Axial CT (A), ^{18}F-FDG PET (B), and fused PET/CT (C) images show a cavitary mass lesion with mild ^{18}F-FDG uptake, measuring approximately 55 mm in the longest axial diameter, with a maximum wall thickness of 6 mm and an SUV_{max} of 4.22 (arrows)
^{18}F-FDG PET/CT: ^{18}F-fluorodeoxyglucose positron emission tomography/computed tomography, SUV_{max}: Maximum standard uptake value

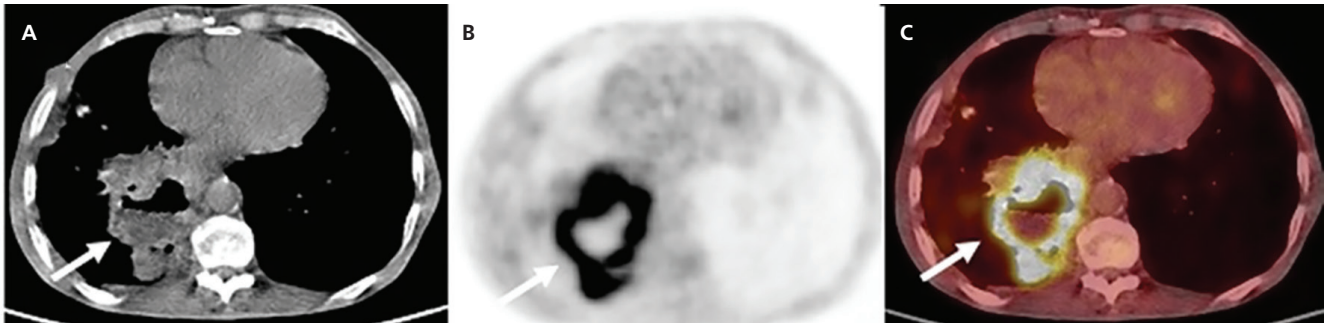

Figure 4. Squamous cell carcinoma. Axial CT (A), ^{18}F-FDG PET (B), and fusion PET/CT (C) images show high ^{18}F-FDG uptake (SUV_{max}: 15.30) on a cavitary mass measuring approximately 93 mm with thick, irregular walls and an internal air-fluid level (arrows)
^{18}F-FDG PET/CT: ^{18}F-fluorodeoxyglucose positron emission tomography/computed tomography, SUV_{max}: Maximum standard uptake value

Table 4. Comparison of SUV_{max} in benign and malignant cavitary lesions based on the maximum wall thickness

	Benign	Malign	p
Maximum wall thickness ≤15 mm, n (%)	23 (30.3%)	13 (17.1%)	<0.001
Maximum wall thickness >15 mm, n (%)	8 (10.5%)	32 (42.1%)	<0.001
SUV_{max}, all lesions, mean ± SD (range)	6.62±4.2 (1.7-21.4)	15.9±7.6 (4.3-30.3)	<0.001
SUV_{max}, maximum wall thickness ≤15 mm, mean ± SD (range)	5.28±2.61 (1.72-11.09)	9.81±7.13 (4.22-25.28)	0.013
SUV_{max}, maximum wall thickness >15 mm, mean ± SD (range)	10.45±5.6 (3.71-21.4)	18.37±6.38 (7.17-30.31)	0.003

Chi-square test for categoric variables, p<0.05 level is significant, Mann-Whitney U test for continuous variables, mean ± SD, p<0.05 level is significant, SD: Standard deviation, SUV_{max}: Maximum standardized uptake value

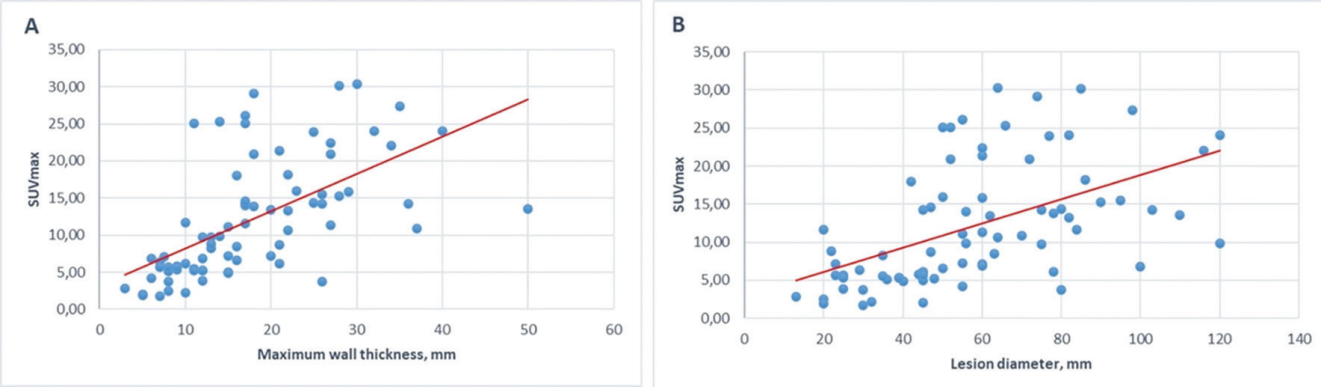

Figure 5. Correlation of SUV_{max} with morphologic parameters. (A) Moderate positive linear correlation between maximum wall thickness (mm) and SUV_{max}. (B) Moderate positive linear correlation between lesion diameter (mm) and SUV_{max}. The red lines indicate linear regression fits
SUV_{max}: Maximum standard uptake value

Table 5. Univariate and multivariate logistic regression analyses in predicting malign cavitary lesion

Parameters	Univariate analysis		Multivariate analysis	
	OR (95% CI)	p	OR (95% CI)	p
Age	1.067 (1.021-1.116)	**0.004**	1.071 (1.008-1.137)	**0.025**
Lesion diameter	1.029 (1.007-1.051)	**0.01**	1.013 (0.96-1.066)	>0.05
Maximum wall thickness	1.15 (1.066-1.246)	**<0.001**	1.00 (0.88-1.12)	>0.05
Presence of air–fluid level	1.48 (0.556-3.963)	0.43	1.009 (0.18-5.6)	>0.05
Presence of pleural effusion	0.715 (0.274-1.867)	0.49	1.853 (0.3-11.22)	>0.05
Presence of perilesional consolidation	0.299 (0.113-0.793)	**0.015**	0.142 (0.018-0.649)	**0.029**
Presence of perilesional infiltration	2.308 (0.888-5.996)	0.086	2.706 (0.547-13.39)	>0.05
SUV_{max}	1.316 (1.153-1.502)	**<0.001**	1.237 (1.039-1.473)	**0.017**

SUV_{max}: Maximum standardized uptake value, OR: Odds ratio, CI: Confidence interval

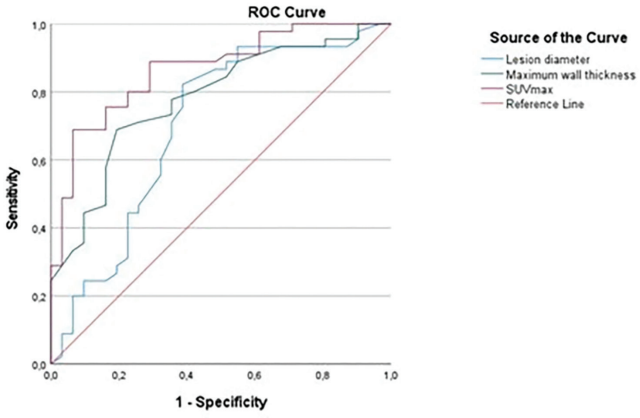

Figure 6. ROC curve analysis showing the diagnostic performance of SUV_{max} (AUC=0.866), maximum wall thickness (AUC=0.78), and lesion diameter (AUC=0.701) for distinguishing benign from malignant cavitary pulmonary lesions
SUV_{max}: Maximum standard uptake value, AUC: Area under the curve

Discussion

Cavitation is observed in approximately 2%-25% of primary lung cancers, with squamous cell carcinoma, adenocarcinoma, and large cell carcinoma being the subtypes most associated with cavitary lesions, respectively (7,8). Differentiating benign from malignant cavitary lesions using radiological imaging methods is a key factor in planning effective treatment strategies. Although CT is the leading imaging technique for detecting cavitary lesions, it can be limited in accurately distinguishing between benign and malignant lesions. CT findings such as multiple cavitary lesions or a tree-in-bud pattern may suggest a benign etiology; however, our results indicate that morphological imaging alone may be insufficient for accurate differentiation. ^{18}F-FDG PET/CT may change preliminary diagnoses based on CT and clinical evaluation. However, some lesions may be misclassified. This situation emphasizes the need to interpret ^{18}F-FDG PET in conjunction with other clinical and imaging information to prevent

misdiagnosis. Our findings showed that ^{18}F-FDG PET/CT imaging can offer valuable insights into the metabolic and morphological characteristics of cavitary lung lesions.

Air space surrounded by a wall less than 2 mm thick is called a cyst (9). Sometimes the cyst wall thickness can reach 4 mm. However, cysts and cavities may not always be distinguishable through radiological imaging. To differentiate, air-filled spaces with walls 4 mm or thinner are referred to as cysts, while those with walls thicker than 4 mm are classified as cavities (10). Wall thickness is one of the most important factors in distinguishing benign cavitary lesions from malignant ones. Woodring et al. (5) reported that in a cohort of 61 patients with cavitary lung lesions, 92% of cavities with a maximum wall thickness ≤4 mm was benign. In lesions with a wall thickness of 5-15 mm, 51% were benign and 49% were malignant, whereas 95% of cavitary lesions with a wall thickness ≥15 mm was malignant. In our study, among the 40 cavitary lesions with a maximum wall thickness >15 mm, a lower rate of malignancy (80%) was observed. Of the 35 cavitary lesions with a maximum wall thickness of 5-15 mm, 13 (37.1%) were malignant. In our ROC analysis, the cut-off point for maximum wall thickness was 15.5 mm for distinguishing malignant cavitary lesions, with a sensitivity of 71.1% and a specificity of 74.2%. Differences in patient selection, underlying disease prevalence, and diagnostic confirmation methods may explain these discrepancies. Although an increase in wall thickness is strongly associated with malignancy, it is not a definitive indicator. There is considerable overlap in the maximum wall thickness between benign and malignant cavities. Thick, irregular walls are often seen in benign cavitary lesions, such as pulmonary abscess, tuberculosis, aspergillosis, and granulomatosis with polyangiitis (2). Conversely, thin walls can also be present in certain malignant cavitary lesions, including adenocarcinoma, squamous cell carcinoma, and cystic metastases from sarcoma and colon adenocarcinoma (10).

It has been shown that perilesional consolidation is more common in tuberculous cavities than in malignant cavitary lesions (3). Consistent with the literature, perilesional consolidation was significantly more common in benign cavitary lesions in our study. We also observed perilesional tree-in-bud nodularity in 25.8% (8/31) of benign cavitary lesions, whereas no perilesional tree-in-bud nodularity was detected in malignant cavitary lesions. The tree-in-bud pattern is characterized by centrilobular micronodules connected to branching linear opacities that resemble a budding tree (11). This finding usually indicates infectious diseases, including bacterial, fungal, viral, or parasitic infections, as well as inflammatory processes such as aspiration and immunologic or connective tissue disorders (12). Primary lung malignancies and metastases—especially those from renal cell carcinoma, breast, liver, stomach, prostate, and ovarian cancers—and Ewing's sarcoma may also present with a tree-in-bud pattern (13,14). However, the presence of a perilesional tree-in-bud pattern supports the diagnosis of a benign cavitary lung lesion (4).

In our study, no significant difference in air-fluid levels was observed between benign and malignant cavitary lesions. This finding is consistent with previous reports indicating that air-fluid levels are nonspecific features and may occur in both infectious cavitary processes and cavitating malignancies due to necrosis, hemorrhage, or secondary infection (2,15).

According to our results, multiple cavitary lesions involving the same lung or the contralateral lung were present in 8 of 31 benign cases (25.8%). No additional cavitary lesions were identified within these malignant cavitary lesions. Primary lung cancer usually presents as a solitary nodule or mass. Lung adenocarcinoma rarely presents as a multiple cavitary disease (16). Multiple metastatic cystic or cavitary lung lesions are reported in colorectal cancer, gallbladder cancer, breast cancer, bladder cancer, renal cell carcinoma, and lymphoma (17,18). However, multiple cavitary lesions are more commonly associated with infectious causes (e.g., abscesses, tuberculosis, fungal or parasitic infections, septic emboli), metastatic disease, or autoimmune conditions such as granulomatosis with polyangiitis, rheumatoid nodules, and vasculitis (1,2).

In our study, a positive correlation was found between SUV_{max} and both cavity size and wall thickness. This relationship reflects the biological aggressiveness of malignant lesions in which necrosis and tumor proliferation coexist. According to our data, cavitary lesions with maximum wall thickness >15 mm showed markedly higher SUV_{max} than those of thinner-walled lesions. Even in cavitary lesions with a maximum wall thickness ≤15 mm, ^{18}F-FDG uptake was higher in malignant lesions than in benign ones. Additionally, SUV_{max} demonstrated good diagnostic performance in distinguishing malignant from benign lesions in our study. At a cut-off value of 8.58, it provided moderate sensitivity (80%) and specificity (77%). Logistic regression analysis showed that higher SUV_{max} values were associated with an increased likelihood of malignancy. This result aligns with the known biological behavior of malignant tumors, which exhibit increased glucose metabolism and ^{18}F-FDG uptake. However, it should be noted that benign infectious and inflammatory cavitary lesions such as tuberculosis or abscesses, can also demonstrate intense ^{18}F-FDG accumulation, potentially leading to false-positive results. Furthermore, thin-walled

cystic or cavitary malignant lesions may show low or absent ^{18}F-FDG uptake. In particular, cystic or cavitary lung adenocarcinomas may show low to moderate ^{18}F-FDG uptake (19). Therefore, SUV_{max} alone cannot be considered an absolute discriminator between benign and malignant cavitary lesions; it should be interpreted in conjunction with morphological characteristics and clinical findings.

Study Limitations

The main limitations were its retrospective design and the relatively small patient cohort from a single institution. Multicenter investigations with larger sample sizes are required to validate SUV_{max} and wall-thickness criteria for the differentiation of cavitary lung lesions.

Conclusion

We concluded that ^{18}F-FDG PET/CT provides valuable complementary information to CT in distinguishing malignant from benign cavitary lung lesions. According to the findings of our study, advanced age and elevated SUV_{max} were significantly associated with a higher likelihood of malignancy, whereas consolidation surrounding the lesion was more frequently observed in benign lesions. Although lesion diameter and maximum wall thickness tended to be greater in malignant lesions, SUV_{max} showed the best performance among quantitative variables in distinguishing malignant from benign lesions. A comprehensive assessment including cavity morphology, wall thickness, lesion size, SUV_{max}, and associated parenchymal findings on ^{18}F-FDG PET/CT can improve diagnostic accuracy and assist clinical decision-making in patients with cavitary pulmonary lesions.

Ethics

Ethics Committee Approval: Ethical approval for this retrospective study was obtained from the Local Ethics Committee of the University of Health Sciences Türkiye, Ankara Atatürk Sanatorium Training and Research Hospital, (approval no: 661, date: 06.02.2020).

Informed Consent: This is retrospective study.

Footnotes

Authorship Contributions

Surgical and Medical Practices: Ö.Ö., E.T., Concept: N.A.D., E.T., Design: Ö.Ö., E.T., Data Collection or Processing: Ü.N.D., N.A.D., Ö.Ö., E.T., Analysis or Interpretation: E.T., N.A.D., Ö.Ö., Literature Search: Ö.Ö., E.T., Writing: N.A.D., Ö.Ö., E.T.

Conflict of Interest: No conflict of interest was declared by the authors.

Financial Disclosure: The authors declared that this study has received no financial support.

References

1. Hansell DM, Bankier AA, MacMahon H, McLoud TC, Müller NL, Remy J. Fleischner society: glossary of terms for thoracic imaging. Radiology. 2008;246:697-722.
2. Parkar AP, Kandiah P. Differential diagnosis of cavitary lung lesions. J Belg Soc Radiol. 2016;100:100.
3. Nin CS, de Souza VV, Alves GR, do Amaral RH, Irion KL, Marchiori E, Hochhegger B. Solitary lung cavities: CT findings in malignant and non-malignant disease. Clin Radiol. 2016;71:1132-1136.
4. Duong TB, Ceglar S, Reaume M, Lee C. Imaging approach to cavitary lung disease. Ann Am Thorac Soc. 2020;17:367-371.
5. Woodring JH, Fried AM, Chuang VP. Solitary cavities of the lung: diagnostic implications of cavity wall thickness. AJR Am J Roentgenol. 1980;135:1269-71.
6. Pinar Deniz P, Duru Çetinkaya P, Hanta İ, Arslan MS, Güney İB. Comparison of ^{18}F-FDG-PET/CT scans in patients diagnosed with sarcoidosis and tuberculosis. Medicine (Baltimore). 2025;104:e41119.
7. Chaudhuri MR. Primary pulmonary cavitating carcinomas. Thorax. 1973;28:354-366.
8. Vourtsi A, Gouliamos A, Moulopoulos L, Papacharalampous X, Chatjiioannou A, Kehagias D, Lamki N. CT appearance of solitary and multiple cystic and cavitary lung lesions. Eur Radiol. 2001;11:612-622.
9. Raoof S, Bondalapati P, Vydyula R, Ryu JH, Gupta N, Raoof S, Galvin J, Rosen MJ, Lynch D, Travis W, Mehta S, Lazzaro R, Naidich D. Cystic lung diseases: algorithmic approach. Chest. 2016;150:945-965.
10. Ryu JH, Swensen SJ. Cystic and cavitary lung diseases: focal and diffuse. Mayo Clin Proc. 2003;78:744-752.
11. Bankier AA, MacMahon H, Colby T, Gevenois PA, Goo JM, Leung ANC, Lynch DA, Schaefer-Prokop CM, Tomiyama N, Travis WD, Verschakelen JA, White CS, Naidich DP. Fleischner society: glossary of terms for thoracic imaging. Radiology. 2024;310:e232558.
12. Miller WT Jr, Panosian JS. Causes and imaging patterns of tree-in-bud opacities. Chest. 2013;144:1883-1892.
13. Li Q, Fan X, Huang XT, Luo TY, Chu ZG, Chen L, Zhang ZW, Li YQ, Wu JQ, Ouyang Y, Lv FJ, Ma CH. Tree-in-bud pattern in central lung cancer: CT findings and pathologic correlation. Lung Cancer. 2015;88:260-266.
14. Bhalla N, Chang CF, Lee C. Special considerations for tree-in-bud nodules. Ann Am Thorac Soc. 2019;16:636-638.
15. Nunes AG, Rodrigues MC, Carneiro C, Costa AC. Pulmonary cavitary lesions: a captivating visual review. J Thorac Dis. 2025;17:6296-6308.
16. Carreto L, Alves C, Eurico J, Cavinho P. Lung adenocarcinoma presenting as a multiple cavitary disease. Arch Bronconeumol (Engl Ed). 2019;55:495-496.
17. Saito T, Kobayashi S, Okutomo K, Miura T, Ohori H, Yanai M. Multiple cavitary lung lesions from colorectal cancer responding to chemotherapy. Respir Med Case Rep. 2023;44:101865.
18. Van Schoor J, Joos G, Pauwels R. Non-Hodgkin's lymphoma presenting as multiple cavitating pulmonary nodules. Eur Respir J. 1993;6:1229-1231.
19. Murota M, Norikane T, Yamamoto Y, Ishimura M, Mitamura K, Takami Y, Fujimoto K, Satoh K, Yokota N, Ishiakawa R, Nishiyama Y. Cystic and cavitary lung cancer: its characteristic features on CT and FDG-PET scans. I J Radiol. 2023;20:e130478.